institut für elektronische musik und akustik

IEM Report 39/07

Icosahedral Loudspeaker Array

Verfasser:

Franz Zotter

Alois Sontacchi

January 2007

A-8010 Graz, Inffeldgasse 10/3, Tel.:+43/(0)316/389 – 3170, FAX:+43/(0)316/389 – 3171

office@iem.at http://iem.at

Zusammenfassung

Herkömmliche Lautsprecherwiedergabe mit einem Lautsprecher kann insbesondere den Aspekt der Synthese von Abstrahlungsformen nicht nachbilden. Einzellautsprecher haben ihre eigene Abstrahlungswirkung, die in Wirklichkeit sehr weit von der Abstrahlung des reproduzierten Instrumentalklangs abweichen kann. Wir haben, um die Abstrahlungssynthese zu ermöglichen, am Institut für Elektronische Musik und Akustik (IEM) ein ikosaederförmiges Lautsprechersystem gebaut. Dieser Bericht dokumentiert den Aufbau davon, die Bestandteile, sowie erste Messungen und Bewertungen, die an dem neuen Gerät vorgenommen wurden.

Abstract

An aspect that can't be covered yet by classical loudspeaker playback is radiation synthesis. In fact, a single loudspeaker will have its own radiation characteristics that can be quite different compared to the radiation of the musical instrument it is used to reproduce with. To accomplish this, we have built an icosahedral louspeaker array system at the Institute of Electronic Music and Acoustics (IEM). This report contains a documentation of its construction, its components, as well as the first measurements and characterizations we have done on this new device.

Contents

1 Introduction **4**

2 Design Considerations **4**

2.1 Driver Design 4

2.2 Enclosure Size, Lower Cut-Off 4

2.3 Driver Spacing, Upper Cut-Off 5

3 Construction Issues **6**

3.1 Preparing and Mounting the Speakers 6

3.2 Cabling and Amplification 7

4 Measurements and Characterization **8**

4.1 Measurement Setup 8

4.2 Impulse Response Windowing 9

4.3 MIMO-Description 10

4.4 Exploiting Symmetric Exchange for MIMO-Description 10

4.5 Desired Radiation Pattern 12

4.6 Normalized Steering Error 13

5 Acknowledgements **15**

1 Introduction

Our institute has done a lot of research in the domain of multichannel holophonic sound reproduction systems. These, especially Ambisonic, are mainly used to reproduce a soundfield environments in a listening room, or in headphone based playback systems, in order to reproduce the incident sound environment at one listening point (cf. Daniel [1]).

In this paper we will consider some kind of inverse application, i.e. the radiation of sound waves from one point with a spherical loudspeaker array (cf. Warusfel *et al.* [2], Kassakian *et al.* [3]).

As described by e.g. Daniel [1], Petersen [4], or Li [5], it is necessary to find a suitable set of nodes on a spherical surface for numerical integration. Considering its simplicity in construction, a given limit in the amount of speakers, and its uniform distribution of points, we chose the icosahedron as basic shape for our spherical array.

The acoustical design criterion for the playback system was the fundamental frequency $f_0 = 42$[Hz] and level of 94dB of the *gong ageng* we want to synthesize with the spherical array. Of course, this is a very low frequency, but we also want to inspect radiation characteristics in room acoustic environments at low frequencies.

2 Design Considerations

2.1 Driver Design

Our speaker array shall be capable of reproducing radiation within a range of approximately 40[Hz] $< f <$ 4000[Hz]. Therefore, we have chosen a coaxial $6\frac{1}{2}$["] and 1["] driver pair with cross over frequency at approximately 2[kHz][1]. We get upper cut-off frequencies for a spherical radiation at $k \cdot r_M = \frac{2 \cdot \pi \cdot f_U}{c} = \pi$, i.e. $f_{U1} \approx 2$[kHz], $f_{U2} \approx 13$[kHz].

2.2 Enclosure Size, Lower Cut-Off

Measured resonance frequencies of an unmounted speaker without and with $m_Z = 5g$ additive mass are (mass difference method, Graber lecture notes [6], Dickason [7], Zwicker [8]):

$$\begin{aligned} f_{oS} &= 59.4\text{[Hz]} \\ f_{oS,Z} &= 50\text{[Hz]}. \end{aligned}$$

For the acutal equivalent membrane mass we get (cf. [6], [7], [8])

$$m_{g,oS} = \frac{m_Z}{\left(\frac{f_{oS}}{f_{oS,Z}}\right)^2 - 1}. \tag{1}$$

[1] All drivers and cross-over circuits were sponsored by ITEC-Audio, Austria

The membrane stiffness becomes (cf. [6], [7], [8])

$$C_{m,Ma} = \frac{1}{m_{g,oS} \cdot \omega_{oS}^2} = \frac{\left(\frac{f_{oS}}{f_{oS,Z}}\right)^2 - 1}{m_Z \cdot \omega_{oS}^2}. \tag{2}$$

Finally, with the given membrane radius $r_M = 6$[cm], we are able to calculate the equivalent volume stiffness of the membrane construction (cf. [6], [7], [8]):

$$V_{a,Ma} = \rho \cdot c^2 \cdot A_M^2 \cdot C_{m,Ma} = \rho \cdot c^2 \cdot r_m^2 \pi \cdot \frac{\left(\frac{f_{oS}}{f_{oS,Z}}\right)^2 - 1}{m_Z \cdot 4\pi^2 f_{oS}^2} \tag{3}$$

In numbers, we have

$$V_{a,Ma} = 1.2 \cdot 340^2 \cdot (6 \cdot 10^{-2})^2 \pi \cdot \frac{\left(\frac{59.4}{50}\right)^2 - 1}{5 \cdot 10^{-3} \cdot 4\pi^2 59.4^2} = 0.011[\text{m}^3] \tag{4}$$

The volume of an icosahedron is (cf. Ortner [9])

$$V = \frac{2}{3}\sqrt{2\left(5+\sqrt{5}\right)} \cdot r^3, \tag{5}$$

for the radius $r = 26.5$[cm], we get $V = 0.047$[m^3].

For a box with $V_B = 0.047$[m^3], we get the lower cut-off frequency (cf. [6], [7], [8]), assuming $f_{uS} \approx f_{oS}$:

$$f_L = 0.93 \cdot \sqrt{1 + \frac{V_{a,Ma}}{V_B}} \cdot f_{uS} = 61[\text{Hz}]. \tag{6}$$

For the closed box, we have a 2^{nd} order high-pass skirt (cf. [6], [7], [8]). For the frequency $f_{\text{Gong}} = 42$[Hz] we get the following attenuation:

$$H(f_{\text{Gong}}) = -10 \cdot \log_{10}\left[1 + \left(\frac{f_L}{f_{\text{Gong}}}\right)^4\right] = -7.4\text{dB}. \tag{7}$$

2.3 Driver Spacing, Upper Cut-Off

We can fit a dodecahedron into our icosahedron to determin the driver spacing. The edges of this dodecahedron connect the centers of the loudspeakers mounted into the icosahedral skeleton. For an icosahedron with (outer) radius $r = 33$[cm] we get the radius of the insphere $r_{in} = r\sqrt{\cdot\frac{7+3\sqrt{5}}{3\cdot\left(5+\sqrt{5}\right)}} = 26$[cm] So the spacing between the speakers corresponds to the edges of the dodecahedron $a = \frac{4\cdot r_{in}}{\left(1+\sqrt{5}\right)\sqrt{3}} = 19$[cm], (cf. Ortner [9]).

Using $\frac{\lambda_l}{2} = \frac{c}{2\cdot f_u} \stackrel{!}{=} a$, we get some upper cut-off frequency for spatial aliasing at $f_u = 1$[kHz]. Nevertheless, in projections onto radial directions, there will always exist

distances smaller than a, so we cannot clearly speak of aliasing for frequencies $f > f_u$. An alternative frequency for aliasing can be given at $f_u = 3$[kHz], selecting a radial direction going through one speaker.

Considering the broadband playback capability of the spherical array system, it is useful to build the speakers into one common enclosure volume. The major drawback, however, is the cross-talk between the speakers over the common enclosure.

3 Construction Issues

3.1 Preparing and Mounting the Speakers

According to the sizes determined above considerations, we have had built an icosahedral skeleton shape out of MDFs (cf. Fig. 1). A loudspeaker stand connector, as well as a multipin connector has been mounted on one of the corners of the icosahedron (see Fig. 4).

Figure 1: The icosahedral skeleton for the loudspeaker array in February 2006.

Between March and May 2006, we have connected the cross-over circuits of the coaxially mounted drivers and glued them on the bass speakers (see Fig. 2).

In May 2006, the speakers have been mounted into the enclosure (see Fig. 3). We filled the enclosure loosly with acoustic damping wool.

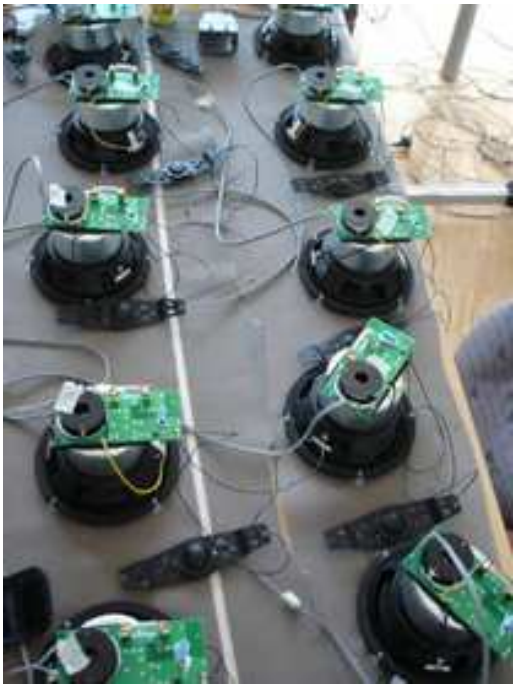

Figure 2: Joining the cross-over circuits with the speaker drivers in April 2006.

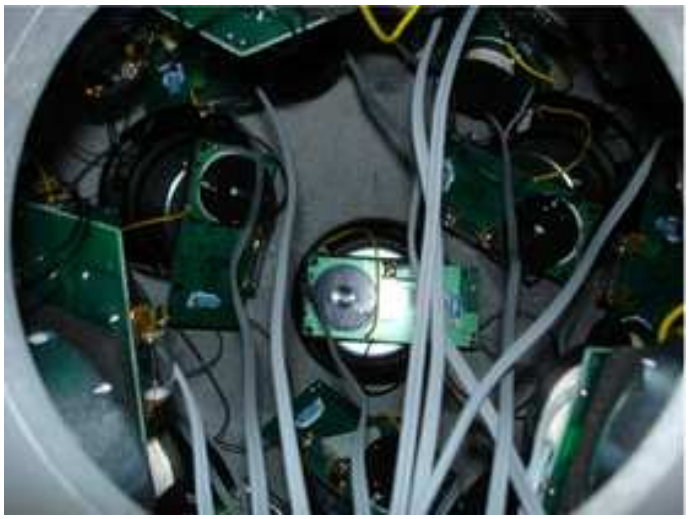

Figure 3: Mounting the speakers in June 2006.

3.2 Cabling and Amplification

We used a 42-pin Multipin-connector for wiring the drivers with the amplifiers, via 13m of 20 ordinary 2.5mm^2 loudspeaker cables. On the other side of the cable, three 8x100W multichannel amplifiers are used (cf. Fig. 4). The signals are obtained from a MADI multichannel audio interface and DA-converters for PC. Our PC is running *pd* (pure-

data) under linux.

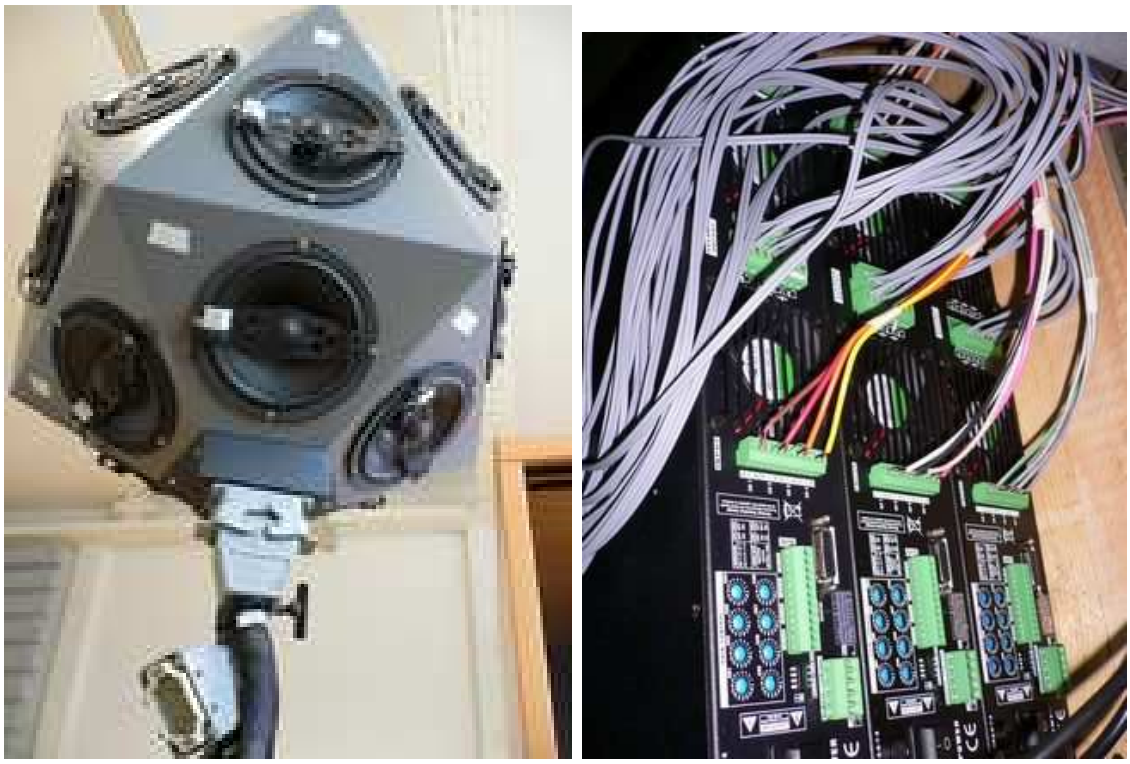

Figure 4: Multipin Connectors and amplifier connections.

4 Measurements and Characterization

4.1 Measurement Setup

For the first few measurements, we used a circular microphone-array in an acoustically damped room (see Fig. 5).

For a preliminary study, we neglected the non-ideal omnidirectional microphone characteristics, and the manufacturing tolerances in the driver properties. Under all these assumptions, we can exploit the icosahedral symmetries. There wer only two measurement series using a ten element circular array of 90° aperture. The speaker array was set up in 0° and 36° orientation for the two measurement series consisting of 400 seperate transfer paths. The 20 measurement points can be expanded to a grid of 172 measurement positions (see Fig. 6). We will explain this a few lines later. We took the measurements using a log-swept sine technique that also delivers some information about nonlinear distortions.

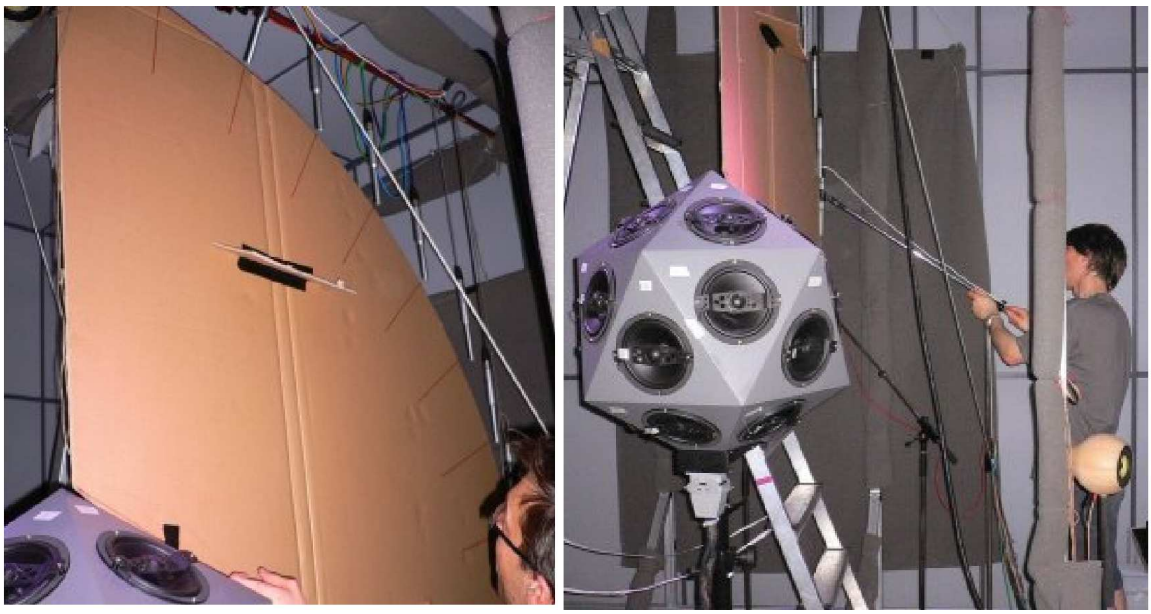

Figure 5: Adjusting the circular array microphones. We disregarded the axial aiming of the microphones.

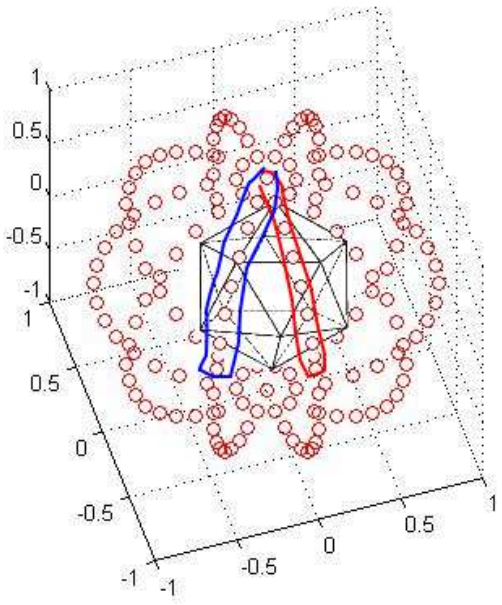

Figure 6: Virtual measurement grid and actually measured responses (highlighted by the pencil strokes).

4.2 Impulse Response Windowing

Due to size and residual reverberation of the measurement room, we had to use windowing techniques to seperate the impulse responses from the room reverberation. An

exponential window starting at 2ms from the direct responses has been applied (see Fig. 7).

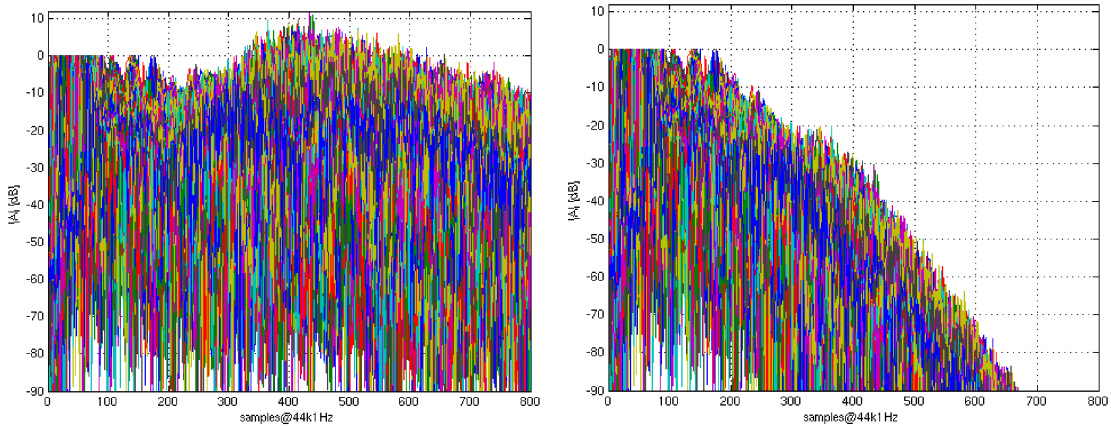

Figure 7: We see the impulse responses on a logarithmic scale, normalized to their first peak each in the first picture. In order to suppress the unwanted acoustic reflexions in the measurement chamber, we apply an exponential window. The skirt of the exponential time-domain window starts at 4ms using -11.25dB/[ms] slope; the resulting attenuation can be seen in the picture below.

4.3 MIMO-Description

For convenience, we work in the frequency domain at a certain freqency ω. With the (Lx1) input sample vector $\mathbf{X}(\omega)$ at the loudspeakers and the (Mx1) output sample vector $\mathbf{Y}(\omega)$ at the microphones,

$$\mathbf{X}(\omega) = [X_1(\omega), \cdots, X_L(\omega)]^t \quad (8)$$

$$\mathbf{Y}(\omega) = [Y_1(\omega), \cdots, Y_M(\omega)]^t, \quad (9)$$

we get a (MxL) MIMO-system $\mathbf{H}(\omega)$, see also Fig. 8:

$$\mathbf{H}(\omega) = \begin{bmatrix} H_{1,1}(\omega), & \cdots, & H_{1,L}(\omega) \\ \vdots, & \cdots, & \vdots \\ H_{M,1}(\omega), & \cdots, & H_{M,L}(\omega) \end{bmatrix}, \quad (10)$$

according to the equation

$$\mathbf{Y}(\omega) = \mathbf{H}(\omega) \cdot \mathbf{X}(\omega). \quad (11)$$

4.4 Exploiting Symmetric Exchange for MIMO-Description

To obtain the entire rectangularly spaced MIMO transfer function matrix, several column and row interchanging operations are allowed due to the symmetries in the arrangement.

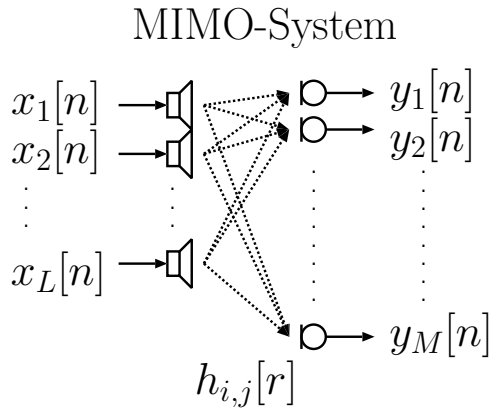

Figure 8: Measurement setup block diagram.

We have measured two cross-sections of the radiated soundfield. All other cross-sections needed (see Fig. 6) can be derived from the two measured by interchanging loudspeaker and microphone indices. A scheme of the icosahedron with numbered surfaces and the microphone cross-sections with microphone numbers is provided in Fig. 9. For the cross-sections at a $36°$ azimuthally shifted position we have to:

1. interchange the loudspeaker indices
   - $[1, 2, 3, 4, 5] \Leftarrow [20, 16, 17, 18, 19]$
   - $[6, 7, 8, 9, 10] \Leftarrow [15, 11, 12, 13, 14]$
   - $[11, 12, 13, 14, 15] \Leftarrow [6, 7, 8, 9, 10]$
   - $[16, 17, 18, 19, 20] \Leftarrow [1, 2, 3, 4, 5]$
2. and invert the microphone order
   - $[1, 2, \ldots, 19] \Leftarrow [19, 18, \ldots, 1]$,

according to the scheme drawn in Fig. 9.

Furthermore, due to the symmetries w.r.t the measurement plane, some responses should be equal, i.e. their loudspeaker indices are interchangeable:

- $[1, 2, 3, 4, 5] \Leftrightarrow [5, 4, 3, 2, 1]$
- $[6, 7, 8, 9, 10] \Leftrightarrow [10, 9, 8, 7, 6]$
- $[11, 12, 13, 14, 15] \Leftrightarrow [14, 13, 12, 11, 15]$
- $[16, 17, 18, 19, 20] \Leftrightarrow [19, 18, 17, 16, 20]$

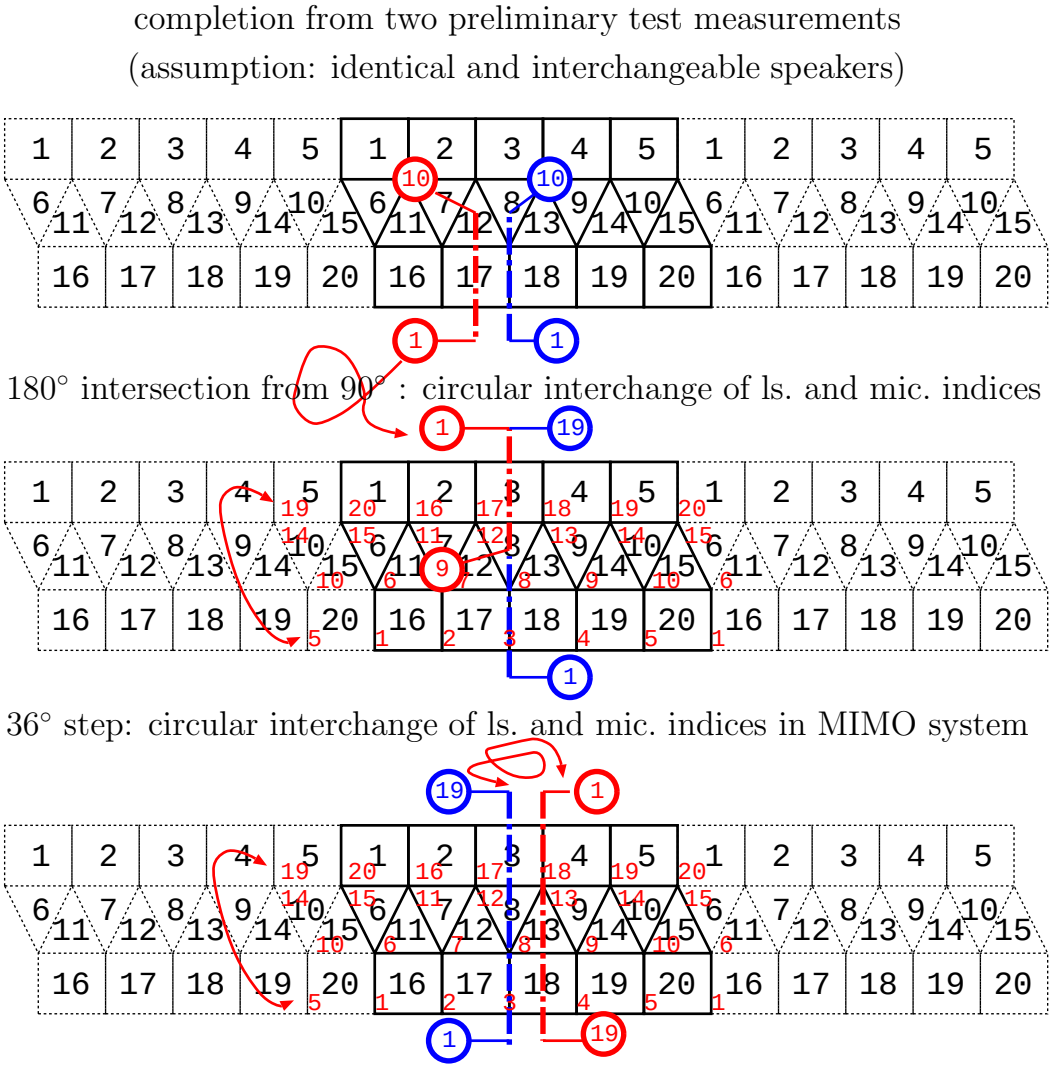

Figure 9: Obtaining the entire MIMO grid from index interchanges due to icosahedral symmetries.

4.5 Desired Radiation Pattern

We want to reproduce arbitrary radiation patterns up to the resolution accomplishable with the icosahedral speaker array. The spherical harmonic functions are an appropriate choice of basis functions. With a given set of $K = (N+1)^2$ spherical harmonics, we can synthesize radiation patterns up to an angular bandwidth N. In the case of the icosahedral loudspeaker array, we are limited to of $N_{ico} = 3$, as the system is determined by $(N+1)^2 \leq 20$ regularly spaced loudspeakers.

To obtain a specific set of K target patterns $\mathbf{B}$ at the microphone positions $(M \times K)$, we have to invert the MIMO-system. This can be done in frequency domain, using the least squares solution[2],

$$\left\| \mathbf{H}(\omega)\, \mathbf{W}(\omega) - \mathbf{B} e^{-j\omega n} \right\|_2^2 \;\rightarrow\; \text{min.} \tag{12}$$

[2] $\mathbf{A}^{\dagger} = \left(\mathbf{A}^{\mathbf{H}}\mathbf{A}\right)^{-1}\mathbf{A}^{\mathbf{H}}$ is the pseudo-inverse of $\mathbf{A}$

$$\mathbf{W}(\omega) \quad = \quad \mathbf{H}^{\dagger}(\omega) \cdot \mathbf{B} \cdot e^{-j\omega \cdot n},$$

where $e^{-j\omega \cdot n}$ is a time-delay of n samples to make the system causal, and $\mathbf{W}(\omega)$ is the $(L \times K)$ set of complex driving weights for the loudspeakers at the frequency ω.

Now, if a target pattern $\mathbf{Y}$ can be decomposed into our base set of target patterns $\mathbf{Y} = \mathbf{B}\lambda$, the following should hold too:

$$\left\| \mathbf{H}(\omega)\, \mathbf{W}(\omega)\, \lambda - \mathbf{B}\lambda e^{-j\omega n} \right\|_2^2 \rightarrow \text{min.} \tag{13}$$

If we want to synthesize a certain signal $x(\omega)$ with the steering vector λ, this is also true:

$$\left\| \mathbf{H}(\omega)\, \mathbf{W}(\omega)\, \lambda x(\omega) - \mathbf{B}\lambda e^{-j\omega n} x(\omega) \right\|_2^2 \rightarrow \text{min.} \tag{14}$$

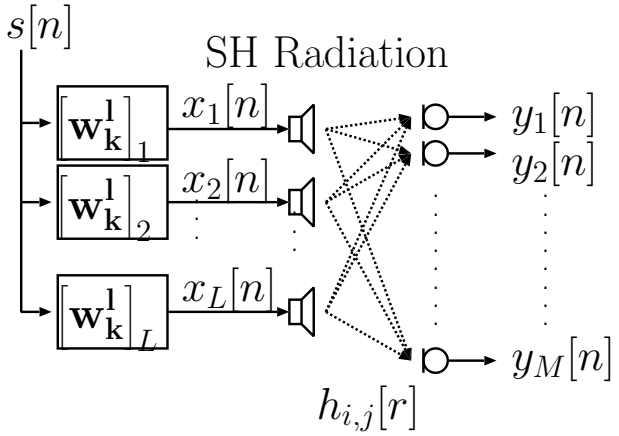

Figure 10: Driving filter block diagram for one single radiation pattern.

4.6 Normalized Steering Error

We can assess the quality of the arrangement by using the relations Peter Kassakian described in [10]. It is, however, decisive that we have to use quadrature weights before we start. As a pre-condition for the assessment, the basis of target patterns has to be orthonormal $\mathbf{B^H B} = \mathbf{I}$. For the spherical harmonics this only holds for a regularly (uniformly) sampled spherical surface, and not for rectangular sampling. Nevertheless, we can approximate orthonormality by using quadrature weights $\mathbf{C}$. For this reason, we desire the following orthonormality relation:

$$(\mathbf{CB})^{\mathbf{H}}\, \mathbf{CB} \stackrel{!}{=} \mathbf{I}. \tag{15}$$

In our case, the system is underdetermined and could only be solved by approximation. An intuitive approach to solve this equation, is to assign weights to each point, according to its equivalent surface fraction. The angular grid here, is defined by $\theta_k = \frac{\pi k}{N_\theta}$, with $k = 0, 1, \ldots, N_\theta$, and $\varphi_l = \frac{2\pi l}{N_\varphi}$ with $l = 0, 1, \ldots, N_\varphi - 1$. The surface of the slice of a

sphere between $\theta_i < \theta < \theta_j$ and its fraction of the whole sphere can be given as (cf. [11], p. 162):

$$S_{\mathsf{sl}} = 2\pi r^2 \left[\cos\left(\theta_i\right) - \cos\left(\theta_j\right)\right], \tag{16}$$

$$\frac{S_{\mathsf{sl}}}{4r^2\pi} = \frac{\cos\left(\theta_i\right) - \cos\left(\theta_j\right)}{2}. \tag{17}$$

Dividing by the azimuthal steps and taking the square root, we get the surface fractions of one single node:

$$c_{k,l} = \begin{cases} \sqrt{\frac{1-\cos\left(\frac{\pi}{2N_\theta}\right)}{2}} & \text{, if } k = 0, N_\theta \\ \sqrt{\frac{\cos\left(\varphi_k + \frac{\pi}{2N_\theta}\right) - \cos\left(\varphi_k - \frac{\pi}{2N_\theta}\right)}{2N_\varphi}} & \text{, else.} \end{cases} \tag{18}$$

Assigning the quadrature weights to the node points, we get the weighting matrix $\mathbf{C} = \mathrm{diag}\left\{\mathbf{c}\right\}$. The result $\left(f\mathbf{CB}\right)^{\mathbf{H}} f\mathbf{CB}$ of this approximative quadrature is shown in Fig. 11. We have also introduced a scalar normalization factor f that normalizes the diagonal elements to unity:

$$f = \sqrt{\frac{\mathsf{trace}\left\{\left(\mathbf{CB}\right)^{\mathbf{H}}\mathbf{CB}\right\}}{K}}. \tag{19}$$

The new weighted least-squares problem considering the quadrature weights $\mathbf{C}$ is:

$$\begin{aligned} \left\|\mathbf{CH}\left(\omega\right)\mathbf{W}\left(\omega\right) - \mathbf{CB}e^{-j\omega n}\right\|_2^2 &\rightarrow \mathsf{min.} \\ \mathbf{W}\left(\omega\right) &= \left(\mathbf{CH}\left(\omega\right)\right)^{\dagger}\mathbf{CB}e^{-j\omega n} \end{aligned} \tag{20}$$

Now we are prepared to derive the normalized steering errors of sub-sets $\mathbf{B_s}$ of the spherical harmonics, sharing the same degree k with the dimension $(M \times 2k+1)$. The procedure can be found in Peter Kassakian's paper [10]. At first we take the QR decomposition of $\mathbf{H}\left(\omega\right)$ $(M \times L)$, with $\mathbf{Q_2}$ $(M \times M - L)$:

$$\left[\mathbf{Q_1}, \mathbf{Q_2}\right]\begin{bmatrix}\tilde{\mathbf{R}} \\ \mathbf{0}\end{bmatrix} = f\mathbf{CH}\left(\omega\right). \tag{21}$$

The normalized steering error bounds for the subset $\mathbf{B_s}$ are determined by the following singular values:

$$\sigma_{\mathsf{min}}\left(f\mathbf{Q_2}^{\mathbf{H}}\mathbf{CB_s}\right) \tag{22}$$

$$\sigma_{\mathsf{max}}\left(f\mathbf{Q_2}^{\mathbf{H}}\mathbf{CB_s}\right), \tag{23}$$

where $\sigma_{\mathsf{min}}\left(\right)$ and $\sigma_{\mathsf{max}}\left(\right)$ denote the minimum and maximum singular values of the matrix in brackets. A diagram can be found in Fig. 11.

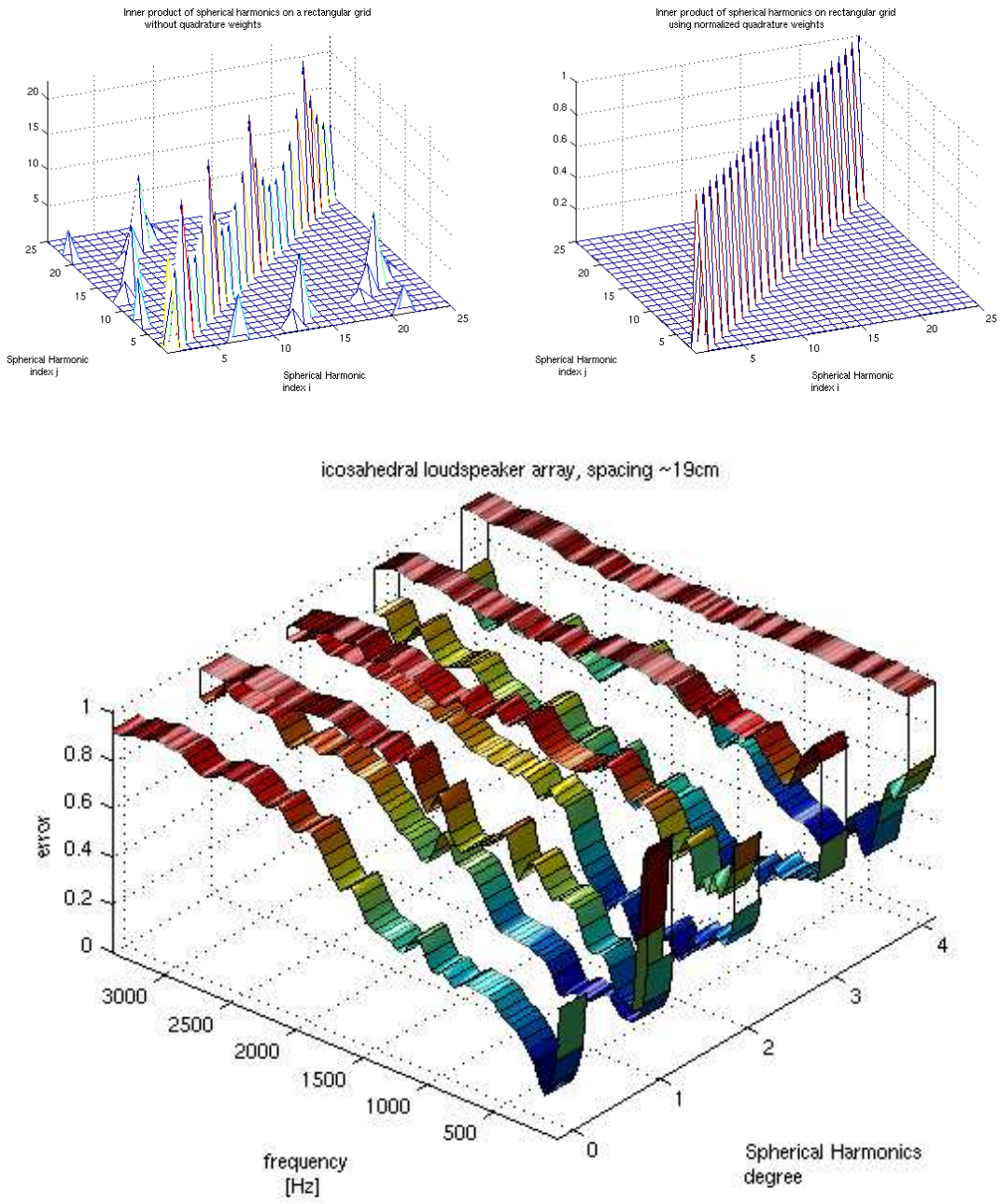

Figure 11: The quality assessment of our icosahedral speaker, following Peter Kassakian's paper [10], is quite poor at the moment. Note that the frequency resolution is reduced by windowing to approximately 220[Hz]. Furthermore, we do know yet, how much deviations arise due to our symmetry assumptions.

5 Acknowledgements

We want to thank Josef Schalk the accurate and dignified construction of the MDF skeleton for our icosahedral speaker system. Christian Jochum and Peter Reiner were a

very diligently filling the skeleton with life, i.e. preparing and mounting of the speakers, cabling, helping through the measurerment of the responses. Furthermore, we are grateful for the characterization scheme by Peter Kassakian, for the speakers from ITEC-Audio and the financial support from the Zukunftsfonds Steiermark.

References

[1] J. Daniel, *Représentation de champs acoustiques, application à la transmission et à la reproduction de scènes sonores complexes dans un contexte multimédia*, PhD thesis, Université Paris 6, France, 2000.

[2] O. Warusfel and N. Misdariis, "Sound Source Radiation Synthesis: from Stage Performance to Domestic Rendering," in *116th AES Convention, May 8-11*, Berlin, Germany, 2004.

[3] Peter Kassakian, "Magnitude Least-Squares Fitting via Semidefinite Programming with Applications to Beamforming and Multidimensional Filter Design," in *International Conference on Acoustics, Speech, and Signal Processing*, IEEE, 2005.

[4] Svend Oscar Petersen, *Localization of Sound Sources Using 3D Microphone Array*, Master's Thesis, University of Southern Denmark, 2004.

[5] Zhiyun Li, Ramani Duraiswami, and Nail A. Gumerov, "Capture and Recreation of Higher Order 3D Sound Fields Via Reciprocity," in *ICAD2004, 6-9 July*, Sidney, Australia, 2004.

[6] Gerhard Graber and Werner Weselak, *Elektroakustik*, IBK Institut für Breitbandkommunikation, TU-Graz, version 5.0 edition, 2001.

[7] Vance Dickason, *Lautsprecherbau*, Elektor-Verlag, 1 edition, 2001.

[8] Manfred Zollner and Eberhard Zwicker, *Elektroakustik*, Springer Verlag, Heidelberg, 3. auflage edition, 1993.

[9] Dieter Ortner, "Die fünf Platonischen Körper," http://www.zebis.ch/inhalte/unterricht/mathematik/polyeder.pdf, Zentralschweizer Bildungsserver, 2003.

[10] Peter Kassakian and David Wessel, "Characterization of Spherical Loudspeaker Arrays," in 117^{th} *Convention of the Audion Engineering Society*, San Francisco, 28-31 Oct. 2005.

[11] I.N. Bronstein and K.A. Semandjajew and G. Musiol and H. Mühlig, *Taschenbuch der Mathematik*, Verlag Harri Deutsch, Thun und Frankfurt am Main, 5. überarbeitete und erweiterte Auflage edition, 2001.